Journal of Visualization, Vol. 4, No. 1 (2001) 39-49

2D Spectral and Turbulence Length Scale Estimation with PIV

Piirto, M.*[1], Ihalainen, H.*[2], Eloranta, H.*[1] and Saarenrinne, P.*[1]

*1 Energy and Process Engineering, Tampere University of Technology, PO Box 589, 33101 Tampere, Finland.
*2 Measurement and Information Technology, Tampere University of Technology, PO Box 589, 33101 Tampere, Finland.
e-mail: mika. piirto@tut.fi

Received 24 October 2000.
Revised 10 January 2001.

***Abstract*:** A new method to apply spatial two-dimensional power spectral density (2D PSD) analysis to the data measured with Particle Image Velocimetry (PIV) has been introduced. Applying the method to a set of the velocity vector fields characteristic turbulence length scales can be estimated. In this method the computation of 2D PSD has been performed to two kinds of pre-processed data. In the first set, the local average has been spatially subtracted (Spatial decomposition) and in the second set the time-average has been subtracted (Reynolds decomposition). In the computation of 2D PSD the 2D FFT with the variance scaling has been used.

Besides 2D spectral analysis this paper uses the distribution analysis of the various turbulence quantities and a structure analysis method to estimate the dimensions of coherent structures in the flow. Another method to analyse turbulence length scales is the estimation of the spatial 2D Auto Correlation Coefficient Function (2D ACCF). All these methods applied side by side to the PIV data increase the understanding of the turbulence, its scales and the nature of the coherent structures.

***Keywords*:** PIV, turbulence, length scale, 2D spectral analysis, 2D, coherent structures.

1. Introduction

Two-dimensional (2D) velocity vector fields measured by Particle Image Velocimetry (PIV) contain 2D spatial information which has not yet been fully taken advantage of in the analysis of the turbulence. Recently, many methods for the turbulence analysis for PIV data have been studied, see e.g. (Adrian et al., 2000; Eloranta et al., 1999; Piirto and Saarenrinne, 1999a; Saarenrinne and Piirto, 2000; Stanislas et al., 1998). Only few attempts concentrate on the spatial 2D analysis of continuous sets. In this paper the main emphasis is on introducing 2D spectral and other 2D analysis tools to investigate the flow phenomena. In all these methods instantaneous velocity vector fields or fluctuation fields computed out of them, like in Figs. 1 and 2, have been analysed. If only one instantaneous field has been analysed, the result describes the length scales in that particular instant. However, if a large enough set of fluctuation fields has been analysed and the results have been combined, it will lead to the understanding of the characteristic length scales in the flow. The analysis methods used in this paper have been 2D Power Spectral Density (PSD), 2D Auto Correlation Coefficient Function (ACCF), the coherent structure scale (CSS) and the distribution of the positive and negative fluctuations.

In this paper two different flow cases, introduced in Chapter 2, have been analysed. Discussions of the decomposition and stationary requirements have been done in Chapter 3. The first test case has been analysed in Chapter 4 with 2D ACCF and in Chapter 5 with 2D PSD. In the second test case the fluctuations have been visualized and distributions calculated together with 2D PSD and CSS. The conclusions have been given in Chapter 7.

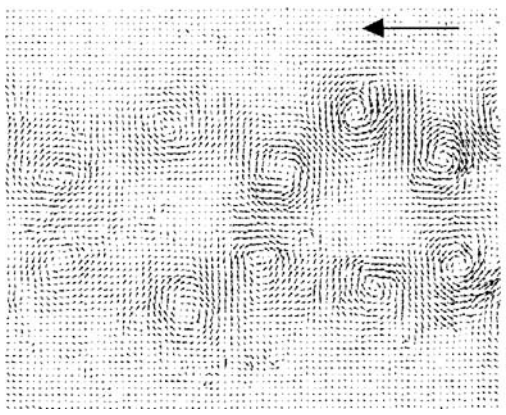

Fig. 1. Spatial fluctuation (average filter / size 25 × 25).

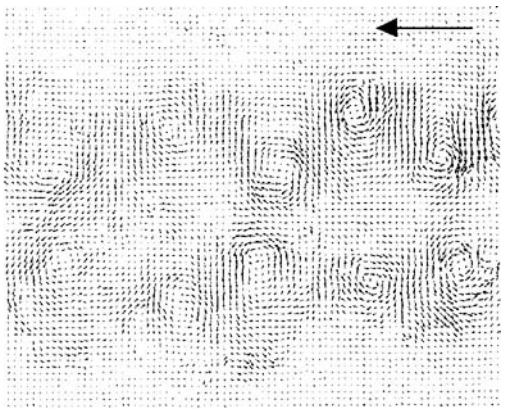

Fig. 2. Time-avg. fluctuation (Reynolds de-composition).

2. Experimental Techniques

Two different data sets have been measured:
1) A channel flow with two parallel flat plates; PIV measurements have been taken just after the plates (x-y -plane) according to the Fig. 3. All dimensions have been normalized by the plate thickness d = 3 mm and the maximum average velocity U_{max} = 7 m/s.

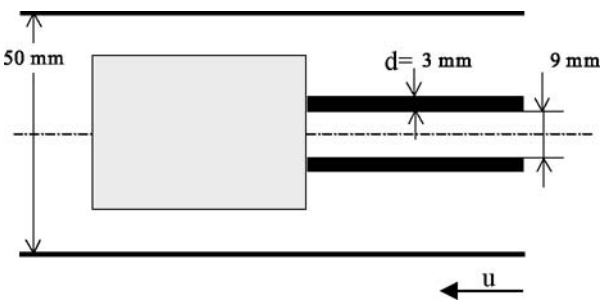

Fig. 3. The case 1 test section (image size) 40 mm × 32 mm is located just after the two flat plates.

2) Near-wall turbulence in a plain channel flow; In this case a plane, parallel to the wall (x-z -plane) at distances y/δ = 0.1, 0.3, 0.5, 0.7 and 0.9 (0.5 mm, 1.5 mm, 2.5 mm, ..., 7.5 mm) have been measured. In wall units the distances are y^+ = 135, 405, 675, 945, 1215. The dimensions have been transferred either into wall units, i.e. normalized by the viscous length scale ν/u_τ or normalized by the boundary layer (BL) thickness δ. The friction velocity has been estimated by fitting the measurement data (streamwise average velocity) to a universal TBL velocity profile of Spalding. For the BL thickness it has been used the criteria $U = 0.99U_\infty$. The flow parameters are

$$Re_\theta = U_\infty\theta/\nu \approx 2900,\ U_\infty \approx 6.45 \text{ m/s},\ \delta \approx 5 \text{ mm},\ \theta \approx 0.45 \text{ mm},\ u_\tau \approx 0.27,\ Re_\tau = 1350$$

For both the cases, the size of the test section (image area) is 40 mm × 32 mm and the vector fields have been computed on 32 × 32 interrogation area with 50% overlapping. Thus, the distance between two adjacent vectors is 0.5 mm, which is about 20-30 times larger for both the test cases than the Kolmogorov length scale approximated with $\eta = (\nu^3/\varepsilon)^{1/4}$ and $\varepsilon = A(u_{rms}^3/l)$, A = 1, as l has been given a value in the order of the integral scale. The integral scale for the streamwise component to the y-direction (test case 1) and to the z-direction (test case 2) has been estimated with PIV and 1D correlation analysis (Piirto et al., 2000) and it is for the test case 1 $l \approx$ 4.4 mm ($u_{rms} \approx$ 0.26 m/s) and for the test case 2 with the distance y/δ = 0.6 from the wall $l \approx$ 3.55 mm ($u_{rms} \approx$ 0.38 m/s). Only turbulence phenomena larger than 20-30 times Kolmogorov length scale can be analysed. If this resolution of 0.5

mm is transformed into the frequency domain by using the Taylors hypothesis and a convective velocity of about 7 m/s (also applicable for both the cases), the maximum measured frequency according to the Nyqvist criteria is about 0.5 × 14000 Hz = 7000 Hz. The fluctuation structures have frequency of about one tenth of this and thus they can be measured quite reliably. Each measured vector field is independent in time because the measurement frequency is low (about 4 Hz). This is important when the measured vector fields have been analysed separately and the results averaged. Only few (1-10) erroneous vectors exceeding the allowed velocity limit have been detected in each vector field of size 78 × 62 vectors. The spurious vectors have been replaced by the interpolation. The measurements have been performed on water seeded by the polyamide particles with average size of 5 μm. The PIV system consists of a Nd: YAG double cavity laser with light sheet optics and a CCD camera of resolution 1280 × 1024 pixels.

3. Decomposition and Stationary Requirements

3.1 Decomposition Methods

Different decomposition techniques show varying performance in detecting and visualizing of coherent structures (CS) in the flow. In Adrian et al. (2000) for example Galilean decomposition, Reynolds decomposition and LES-decomposition (spatial filtering) have been compared and tested to an instantaneous turbulent velocity field. Galilean decomposition will easily leave certain constant velocity component to the flow and is not appropriate for the 2D spectral analysis. According to Adrian et al., from the point of view of visualization, the spatial filtering is the most effective way to discover the small-scale structures. In Fig. 1, an instantaneous velocity vector field has been filtered with a spatial average filter of size 25 × 25 vectors and the results have been subtracted from the original velocity vector field. This is called spatial fluctuation, whereas Reynolds decomposition is called a time-average fluctuation. As can be noticed in the spatial fluctuation field of Fig. 1, rotating eddies are even better visible than in the Reynolds decomposition of Fig. 2. Even though the visualization of the CSs in the test case 1 with the spatial filtering seems to be better, there remains constant streamwise velocity component affecting difficulties in PSD analysis. For this reason 2D PSD analysis has to be performed in time average fluctuations in the test case 1.

Spatial filtering can be performed by giving equal weight to all the operational area of the average filter or by giving more weight to the center of the filter e.g. by using Gaussian type weighting function. On the edge and the corners of the vector fields, the filtering has been optimized to the available data. A special software toolbox for these kinds of fluctuation and filtering operations has been introduced in Piirto et al. (2000) and recently updated making it possible to use any size of the spatial filter to both the directions x and y of 2D vector data. Round shaped or even elliptic type of filters together with the Gaussian weighting can be used, but the research of their effect is still in process. In spatial filtering, the size of the filter defines the maximum size of the flow structures and works as low-pass filter. After subtracting the filtered field from the original one, small-scale structures remain in the resulting high-pass field. For this reason, the size of the spatial filter size is important in the analysis of the "right" scales and the frequencies in the flow. In the second test case the spatial filtering discovers structures, which stay hidden in the time average fluctuation.

3.2 Stationary Requirements

In the turbulence length scale research the analysed area should be defined so that the turbulence length scales remain as constant as possible in that particular analysed area of the flow (Piirto and Saarenrinne, 1999b). If they do not, it is impossible to say which flow phenomenon is behind a particular length scale and in what extent. In the computation of the ACCF and PSD, the stationary requirements should be fulfilled at least in the sense of time-mean and RMS. Practically, this means that the flow properties should be kept constant in the measured region. One easy way to evaluate the stationary level of the data is to divide measured vector fields in four sub-regions of the same size like in Fig. 4. After computing the time-mean and the RMS for the regions, it is possible to compare the results with each other and to the original undivided region. If time-mean or RMS varies a lot, probably the physical conditions have been changed or an error has occurred during the measurement procedure. Naturally, changes due to the boundary conditions like acceleration may change the average value from region to region without affecting Reynolds decomposition and the spectral estimates.

Before the stationary test, it is of course important to make sure the data set is statistically large enough. In this example of computing 2D ACCF after the two flat plates, the data set of 80 vector fields is statistically a bit

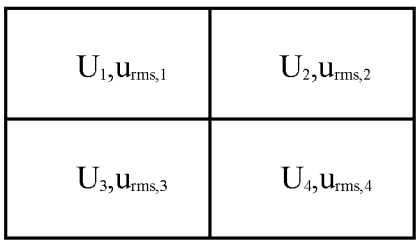

Fig. 4. Measurement area divided in four sub-regions for the stationary test.

too small for the average. Stable values for the average especially close to the tips of the plates will not be reached. For the RMS, the data set is large enough to give stable RMS values. The computational area defines also the available computational data and the maximum length scale, which can be investigated.

4. 2D Autocorrelation Estimate

The computation of the Auto Correlation Coefficient Function (ACCF) estimate is a very classic way to evaluate the length scales of the flow (Hinze, 1975). The advantage of the 2D ACCF is the possibility to measure the correlations to any arbitrary direction on the measurement plane (see e.g. Stanislas et al., 1998). In order to study the characteristic length scales of the particular flow, an large enough set of data has to be analysed. The computation of the 2D ACCF for the time series of Reynolds decomposed PIV vector fields uses the unbiased estimate, which is scaled by the RMS as presented in Eqs. (1) and (2). The RMS values scale the ACCF to value 1 with the zero lag. This scaled ACCF is often called autocovariance. Indexes i and j define the computational area of the flow with a maximum size $p \times q$. The 2D ACCF is symmetric through the origin and the Eqs. (1) and (2) define the two quarters which are identical to the other quarters 3 and 4. Variables Δi and Δj correspond to the correlation lags in x and y direction, respectively.
For the positive lag values the estimate is:

$$\hat{r}(\Delta i, \Delta j) = \frac{1}{(p-\Delta i)(q-\Delta j)n} \sum_{i=1}^{p-\Delta i} \sum_{j=1}^{q-\Delta j} \sum_{\xi=1}^{n} \left[\frac{u'(i,j,\xi) \cdot u'(i+\Delta i, j+\Delta j, \xi)}{u_{rms}(i,j) \cdot u_{rms}(i+\Delta i, j+\Delta j)} \right] \tag{1}$$

With the lags $\Delta i \geq 0, \Delta j < 0$ the estimate is:

$$\hat{r}(\Delta i, \Delta j) = \frac{1}{(p-\Delta i)(q+\Delta j+1)n} \sum_{i=1}^{p-\Delta i} \sum_{j=-\Delta j}^{q} \sum_{\xi=1}^{n} \left[\frac{u'(i,j,\xi) \cdot u'(i+\Delta i, j+\Delta j, \xi)}{u_{rms}(i,j) \cdot u_{rms}(i+\Delta i, j+\Delta j)} \right] \tag{2}$$

In Fig. 5, 2D ACCF has been computed for the streamwise velocity component of the test case 1. The zero lag peak has not been plotted in order to get the other peaks more visible in this color map. Thus, the figure has been scaled from −0.3 to 0.3. In the ACCF map presented in Fig. 5, the angle of 45 degrees is explained by the streamwise fluctuations phase difference. This phenomenon can be noticed in Figs. 1 and 2. Two reciprocal eddies of the instantaneous fluctuations are located with each other in that specific angle. The dominating length scale to the streamwise direction is about 4.5d and to the spanwise direction about 5d. Later it can be noticed that these scales are similar to the scales analysed by 2D PSD. The computation of the Eqs. (1) and (2) can be performed by FFT-autocorrelation algorithm if the velocity vector fields have been pre-processed first. First the time-average fluctuation fields have to be computed and then each one of them has to be scaled with the RMS field. These scaled fields are used as the input data for the FFT-autocorrelation algorithm.

Another advantage of the ACCF method is the simple interpretation of the streamwise and spanwise length scales. It is easy to read the distance to both the directions and check the correlation value in that particular position. However, in most cases the resolution of the PIV vector fields does not allow an accurate estimation of the Taylor micro scales. The estimate of the integral length scale, which in 2D ACCF is the integrated absolute volume of the 2D ACCF map, gives an estimate to the length scale of a typical structure (Hinze, 1975). The interpretation of the integral scale often needs the ACCF map to be plotted beside it, because the integral scale cannot alone describe the correlation on the different length scales. Because the ACCF of Fig. 5 does not reach zero, the total integral scale in this test case remains uncertain. To correct this, the size of the measurement area

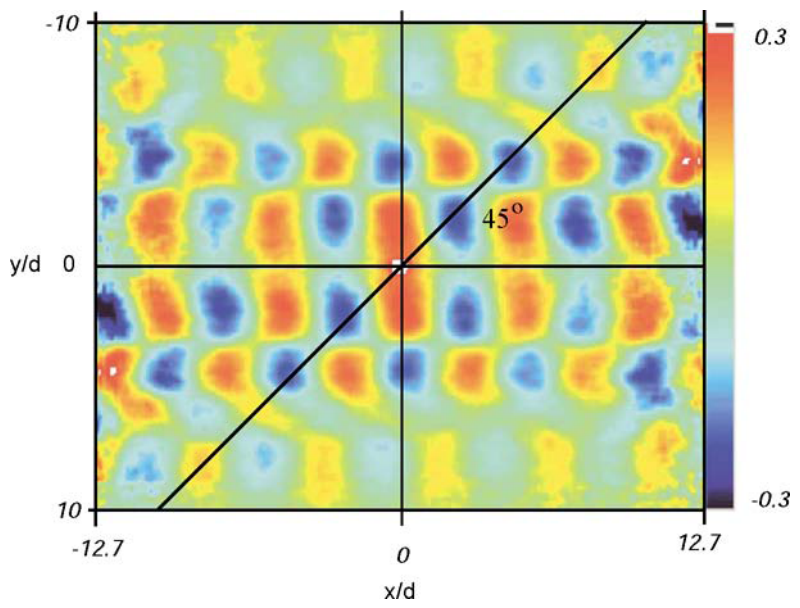

Fig. 5. 2D ACCF map computed for u-component.

should be increased. The procedure used to compute ACCF can be modified to the computation of CCF as well.

5. 2D Spectral Analysis

The 2D spectral analysis method enables the computation of the power spectrum and thus the estimation of the turbulence length scales to all the directions between the main-axis in the resulting 2D PSD map. Constant velocities and generally constant components or trends in the signal (average or trend not removed) makes it more difficult for PSD analysis to find the spectral frequencies. Typically in the turbulence length scale analysis the average has been removed in the decomposition phase of the data. The estimate can be computed by 2D Fast Fourier Transform (2D FFT), like in this example of test case 1, or other PSD methods. Like 2D ACCF, 2D PSD is symmetric through the zero frequencies (f_x, f_y) and thus only two quarters have to be plotted and investigated.

5.1 2D PSD Analysis for Instantaneous Fluctuation Fields

The method for the computation of the two-dimensional FFT is well known and it has been explained in the spectral analysis literature like Marple (1987). In order to test the 2D PSD method, a test eddy in Fig. 6(a) has been cropped from the fluctuation field and analysed with the 2D PSD. Resulting 2D PSD maps have been plotted in Figs. 6(b) and 6(c). As can be noticed, the eddy of a size about 3d can be found in both the 2D PSD maps as peaks at the frequency of about 0.3 (non-dimensionalized by the thickness of the plate 3 mm). The zero frequency means that the eddy contains almost constant velocity components to x-direction of the streamwise fluctuations and similarly to y-direction of the spanwise fluctuations i.e. there is no spectral frequency to be found. These almost constant velocities can be observed also in the eddy of Fig. 6(a). A little bit unsymmetrical velocity profiles in the eddy causes the asymmetry in the 2D PSD maps. Even though the size of the eddy can be read easily from the 2D PSD maps, the vector fields having many eddies with rotation to different directions cause PSD peaks as well. These peaks are caused by the distances of the reciprocal eddies. Depending on the rotation direction, the distance of two reciprocal eddies will become either doubled or halved. All this means that the length scales of the PSD map include both the eddy size and their distance information which both together define the spectral power on different scales.

5.2 Averaged 2D PSD Analysis

For the estimation of the characteristic length scales, the 2D PSD maps computed for the fluctuation fields will be averaged. This method will reveal those length scales, which dominate in the set of analysed fluctuation fields. After the averaging operation, the averaged PSD field has been variance scaled i.e. the volume of the PSD map has been scaled to be equal to the variance of the fluctuations. The whole procedure for streamwise fluctuation

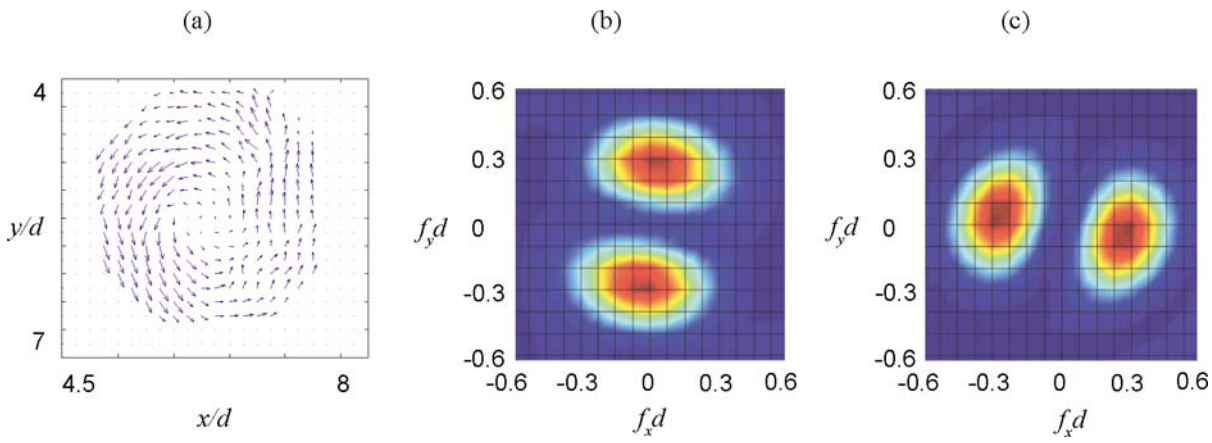

Fig. 6. A test eddy (a) and its 2D PSD maps for u-velocity component (b) and v-velocity component (c).

component is following: 1) Compute 2D FFTs for n fluctuation fields and average computed 2D FFT fields

$$F_{i,j}(u) = \frac{1}{n}\sum_{\xi=1}^{n} 2\mathrm{DFFT}(u_\xi) \tag{3}$$

2) Compute the variance for all the time and spatial components of u and calculate the scaling factor s

$$s = \frac{Var(u)}{dxdy\sum_{i=1}^{p}\sum_{j=1}^{q} F_{i,j}(u)} \tag{4}$$

in which dx and dy are the resolutions of the computed 2D FFT map. 3) Finally compute the variance scaled 2D PSD by using the scaling factor.

$$P_{i,j}(u) = s \cdot F_{i,j}(u) \tag{5}$$

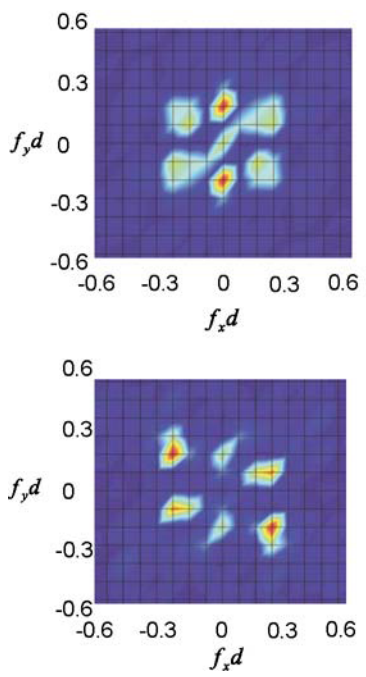

Fig. 7. An example of 2D PSD maps calculated for the instantaneous fluctuation fields of the streamwise velocity component.

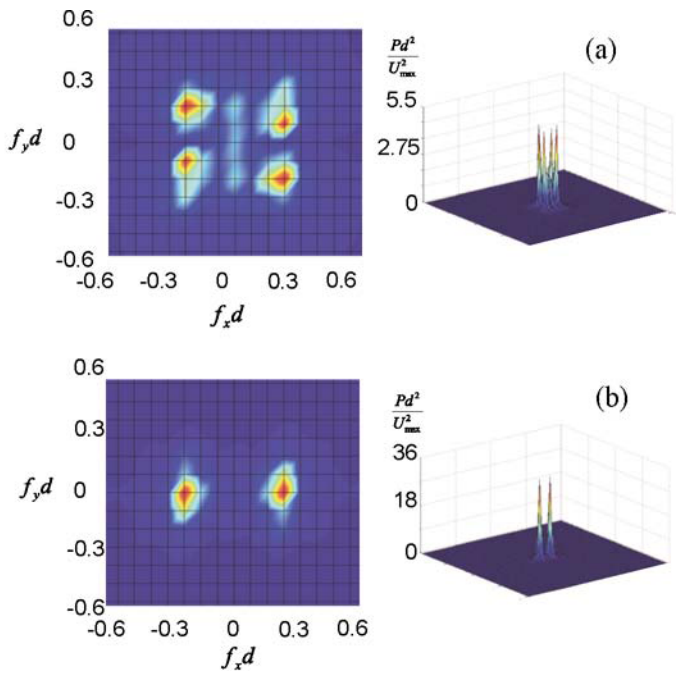

Fig. 8. Averaged 2D PSD map computed for time-average fluctuation fields of the streamwise velocity component (a) and of the spanwise velocity component (b).

In Fig. 8 the averaged 2D PSD estimate has been solved for 80 time-average fluctuation fields. The length scale to the main flow direction is about 4.5d for both fluctuation velocities u and v. In practice, this means the distance of the reciprocal eddies to the streamwise direction. The length scales in Fig. 8(a) to the direction y for the streamwise fluctuation Fig. 8(a) are about 5d and 10d. The length scale of about 10d is the maximum and besides the y-size of the whole fluctuation field. It means that the streamwise fluctuation component to the direction y gets positive values and negative values only once in that distance. The length scale 10d describes the most distant eddies to the direction y whereas the length scale 5d describes the eddies closest to each other. Thus 2D PSD explains the interaction of the fluctuations between the upper and the lower plate: the scale to the direction x is 4.5d whereas the scale to the direction y is either 5d or 10d.

In the instantaneous analysis, the characteristic spectrum peaks can be weak or the disturbances can cause misinterpretation of the characteristic length scales. However, it is always suggested to open the research with the spectrums for the instantaneous vector fields before using the averaging of the spectrums. This will give an idea what kind of length scales generally exist in the flow. In Fig. 7, two 2D PSD maps have been solved as an example for instantaneous vector fields of the streamwise fluctuation. As can be noticed, the 2D PSD maps for the instantaneous fluctuation fields are very different from each other. In the results one must be careful not to explain the spectral peaks only as the size or as the distance of the coherent structures but rather with the size and the distance combined.

6. Near-wall Turbulence Analysis

The next flow case is near-wall turbulence in a plain channel flow introduced in Chapter 2. The near-wall turbulence has been studied with PIV e.g. by Tomkins and Adrian (2000), Kähler et al. (1998), Stanislas et al. (1998) and Meinhart and Adrian (1995). The first two papers study near-wall turbulence in the x-z plane and the last two papers in the x-y plane on different distances between y^+ = 20-200. According to Tomkins and Adrian (2000) and Kähler et al. (1998) the scales for the streamwise component to z-direction are in the order of λ_z^+ = 100-600. As shown by Tomkins and Adrian. the most energy (cumulatively 75%) is on the scales larger than λ_z^+ = 100 when the distance from the wall is y^+ = 21 (Re_θ = 1015, Re_τ = 425).

The idea of the length scale analysis in this example is to analyse coherent structures at various distances (y^+ = 135, 405, 675, 945, 1215 or y/δ = 0.1, 0.3, 0.5, 0.7, 0.9) from the wall. Unfortunately Re_θ = 2900 and Re_τ = 1350 are not the same with Tomkins and Adrian (2000). The experimental set-up of this test case 2 with the measurement plane size of $8\delta \times 6\delta$ (x-z) is able to capture relatively large scales. The thickness of the laser-sheet is about 1 mm. The first distance y/δ = 0.1 is defined to be in the middle of the laser sheet thickness.

Spanwise profile (z-direction) for the streamwise fluctuation in Fig. 9 gives an idea about the length scale analysis. Both the structure width and the distance together define one cycle in the PSD analysis. The average profile is shown in Fig. 10. The boundary layer thickness δ is about 5 mm. All the analysis has been applied to the streamwise fluctuation component.

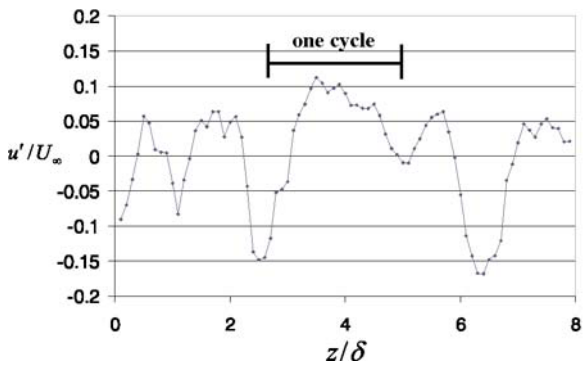

Fig. 9. An example of the z-profile for the streamwise fluctuation component at the distance y/δ = 0.7 from the wall.

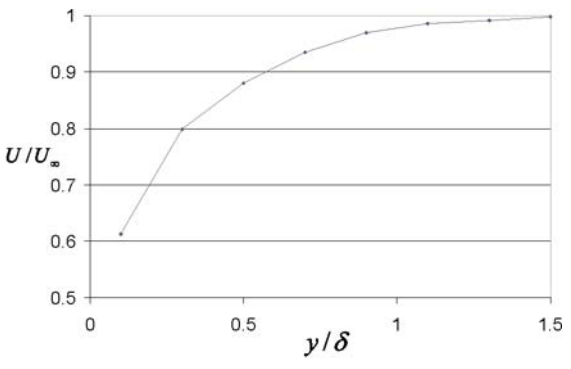

Fig. 10. Streamwise velocity (averaged).

6.1 Effect of Spatial Filtering to PSD

The effect of spatial filtering to PSD has been tested by varying the size of the filter. The filtered velocity field has been subtracted from the original velocity field. These operations (filtering and subtracting) work as a high-pass filter and constant velocities are spatially filtered away. The smaller the size of the filter, the smaller the length scales can be discovered. In Fig. 11 the spatial average filter sizes $2\delta \times 2\delta$, $3\delta \times 3\delta$, $4\delta \times 4\delta$ and the time-average fluctuation have been tested. If the peaks of Fig. 11(b) are compared to the PSD peaks of the time-average fluctuation of Fig. 11(d), the length scales 1.3δ (0.75) and 2.0δ (0.5) can be noticed, but accurate locations of the peaks remain indistinct. Very strong PSD peak at 8δ (0.125) of Fig. 11(d) makes it difficult to locate the other peaks. The variances calculated to the streamwise fluctuations (of all the fields) with the different filter sizes $2\delta \times 2\delta$, $3\delta \times 3\delta$ and $4\delta \times 4\delta$ are 0.08, 0.13 and 0.15 respectively. For the time-average fluctuation it is 0.26, which means less filtering compared to the spatial ones.

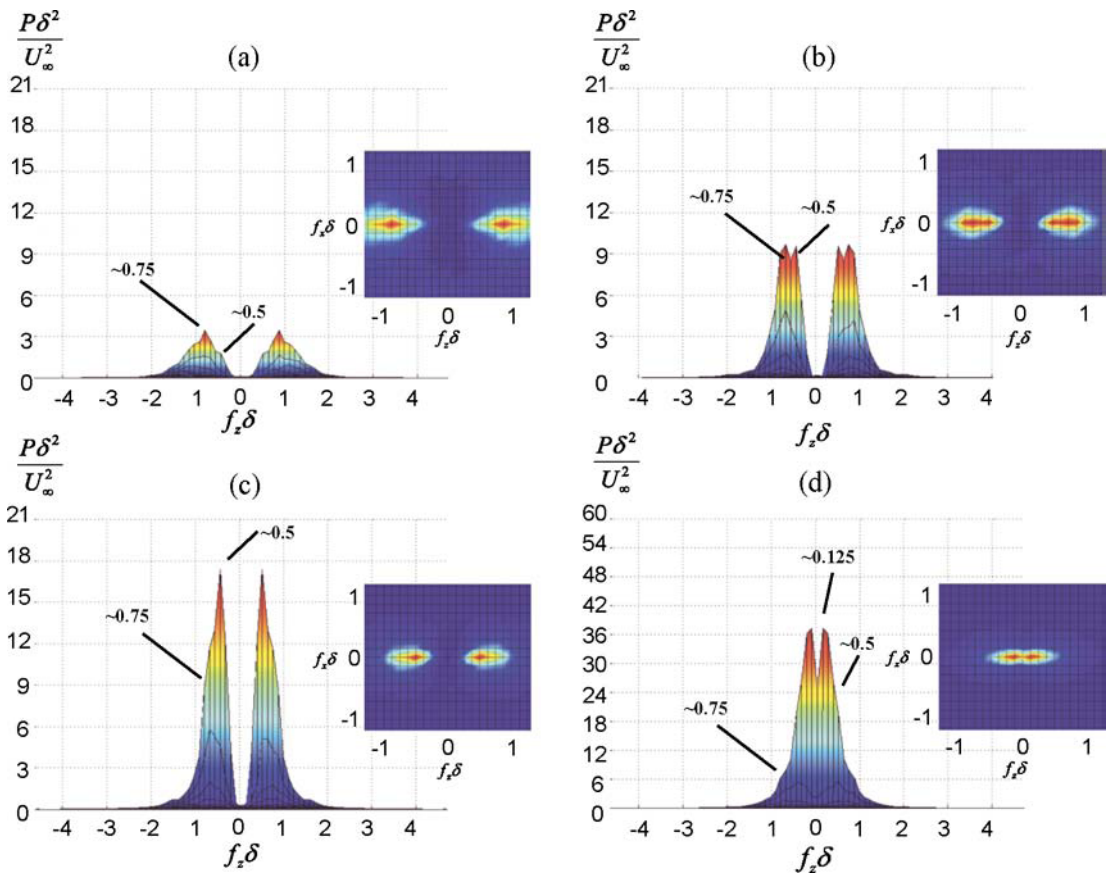

Fig. 11. The effect of the spatial filtering with the different filter sizes (a) $2\delta \times 2\delta$, (b) $3\delta \times 3\delta$, (c) $4\delta \times 4\delta$ to the 2D PSD in comparison to (d) 2D PSD of the time fluctuations (distance $y/\delta = 0.5$).

6.2 Visualization, Distribution, Structure Width and 2D PSD Analysis

In Fig. 12 instantaneous fluctuations of the streamwise component (1), distributions of the fluctuations (2), coherent structure scales (CSS) to z-direction (3) and 2D PSD maps (4) have been plotted side by side with the different distances (a) $y/\delta = 0.1$, (b) $y/\delta = 0.3$, (c) $y/\delta = 0.5$, (d) $y/\delta = 0.7$, (e) $y/\delta = 0.9$ from the wall. 2D PSDs have been computed after the spatial filtering ($3\delta \times 3\delta$) of the vector fields, and 2D PSDs have been averaged and variance scaled according to the Eqs. (3)-(5). The instantaneous time-average fluctuation fields (1) are samples for each distance but the distributions (2) and the CSS (3) have been calculated out of all the 80 fluctuation fields.

In the distribution analysis (2), all the velocity fluctuations have been divided to the different velocity classes thus creating the probability density function.

In the computation procedure of the CSS (3), the time-average fluctuation fields have been scanned line by line. When the fluctuation passes the user-defined threshold level, it increases the counter of that specific width.

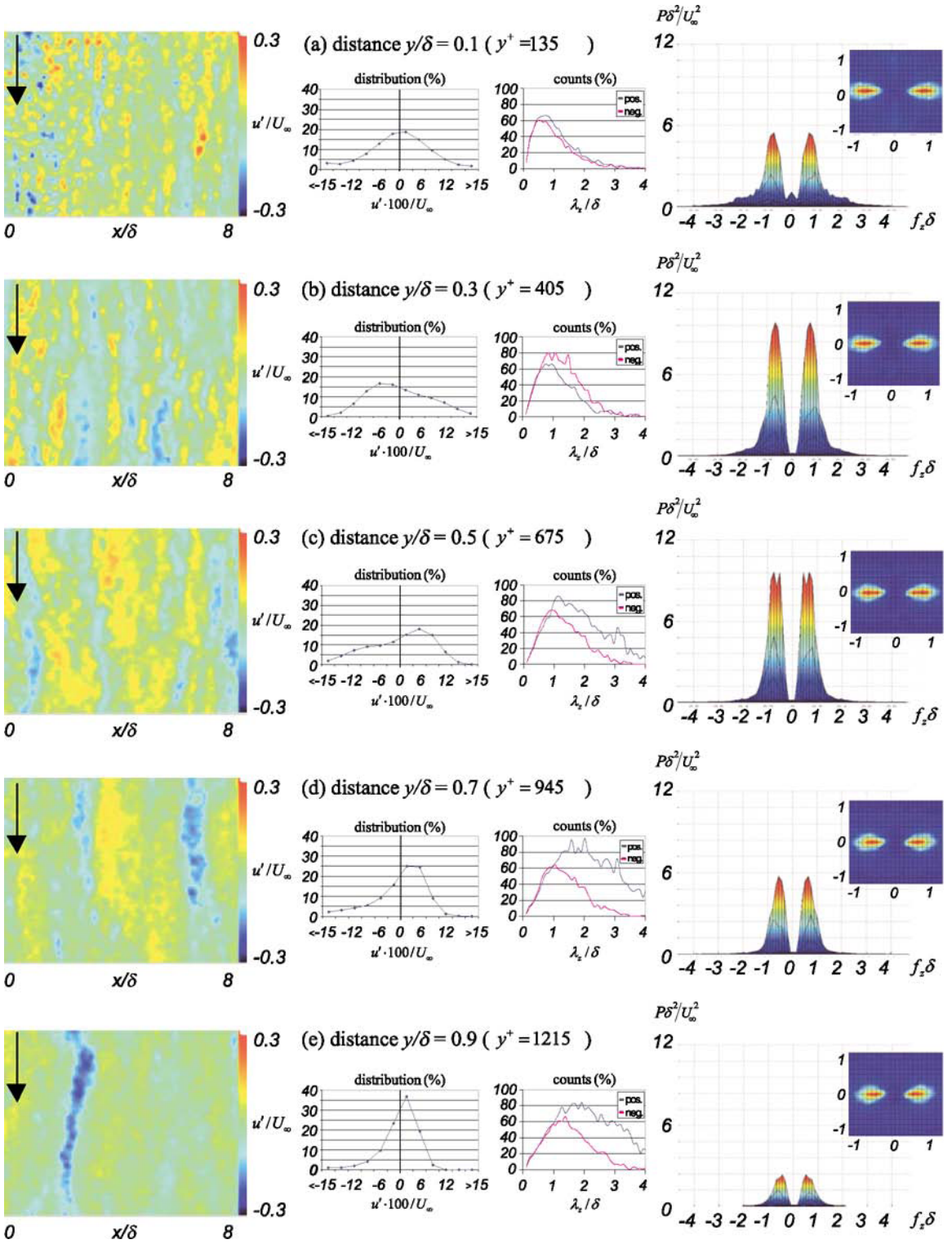

Fig. 12. Near-wall turbulence analysed on the different distances from the wall (a) y/δ = 0.1, (b) y/δ = 0.3, (c) y/δ = 0.5, (d) y/δ = 0.7, (e) y/δ = 0.9 to the streamwise velocity component (up to down in the fluctuations). In figure from left to right (1) time-average fluctuations, (2) distribution of the time average fluctuations, (3) scales (z-direction) of the time-average fluctuations and (4) projection of 2D PSDs of spatial fluctuations (side and top view).

In this analysis case the threshold level has been set 0 m/s, which means that the widths of the positive fluctuation structures have been analysed. The same procedure has been performed for the negative ones. Instead of plotting straightaway the counts of the scales, the counts have been weighted by the size of the structures. This procedure

will help to give less emphasis on the large number of the short structure scales 0.1δ or 0.2δ. The weighting has been accomplished with the fictitious fluctuation structure of the cylindrical shape which total cross-sectional area is: "counts $\times \pi r^2$". Here "r" (radius) is half the CS width (diameter) and "counts" represents the number the particular width found in the analysis.

As can be noticed in the analysis methods (1)-(3) of Fig. 12, the relation of the fluctuations to the distribution analysis and the CSS is obvious. For example, the CSS of the positive fluctuations increases from the distance $y/\delta = 0.3$ and $\lambda_z/\delta = 1$ to $y/\delta = 0.9$ and $\lambda_z/\delta = 2$, which can also be noticed in the contours of the fluctuation fields. The negative fluctuations keep almost the same length scale $\lambda_z/\delta = 1$ at all levels except $y/\delta = 0.1$. With the distance $y/\delta = 0.1$ both the negative and the positive CSSs seem to be in the same size 0.5δ ($\lambda_z^+ \approx 675$). The number of the analysed fluctuation fields could have been higher which may have lead to a little bit smoother curves for the z-scales.

Another remark is that the distributions of the fluctuations do not stay centred to origin and for example on the level $y/\delta = 0.3$ the peak is on negative (about –6%) and by contrast on the level $y/\delta = 0.5$ it is positive (about 6%). There are especially strong negative fluctuations of strength > –12 ... –15% on the distances $y/\delta = 0.7$ and $y/\delta = 0.9$.

With the PSD peaks of the level $y/\delta = 0.5$, the length scales $\lambda_z^+ = \lambda_z u_\tau/\nu$ of the coherent structures are $\lambda_z^+ \approx 2700$ (2δ) and $\lambda_z^+ \approx 1750$ (1.3δ). These scales seem to be in good agreement with the CSS of the positive fluctuation. Closer to the wall than $y/\delta = 0.5$, $\lambda_z^+ \approx 1750$ is the dominating length scale and with the distances $y/\delta > 0.5$, the scale $\lambda_z^+ \approx 2700$ is the most energetic. The interpretation of the PSD length scales is not the width of the streaks but rather the width added to the reciprocal distance of two streaks together as seen in Fig. 9. Most energetic length scales are found in this example at the distances $y/\delta = 0.3$ and $y/\delta = 0.5$ from the wall.

7. Conclusions

2D spectral and autocorrelation methods are effective tools to estimate the turbulence length scales and the spectral power to all the directions of the PIV-velocity vector field. Averaged spectrum reveals the characteristic scales of the flow whereas spectrums for the instantaneous vector fields may discover different length scales. Instead of the size of the structure, the spectral analysis rather reveals the length scale, which is a combination of the structure size and the distance between two reciprocal structures.

The spatial average filtering, used for the computation of the spatial fluctuations, is able to find structures, which may stay hidden after the conventional Reynolds decomposition. With 2D spectral analysis, applied to the spatial fluctuation data, the length scales of the discovered structures can be analysed. Even so, the size for the spatial filter has to be based on the knowledge of the fluctuation structures of the flow.

Visualization of the structures, the size analysis and the distribution analysis for the instantaneous fluctuations or the other instantaneous turbulence quantity fields, reveal information which may improve the analysis of turbulence length scales and coherent structures besides 2D spectral analysis.

References

Adrian, R. J., Christensen, K. T. and Liu, Z. C., Analysis and Interpretation of Instantaneous Turbulent Velocity Fields, Experiments in Fluids, 29 (2000), 275-290.

Eloranta, H., Piirto, M. and Saarenrinne, P., Detection and Visualization of Large-scale Turbulence Using PIV Vector Fields, 3rd International Workshop on Particle Image Velocimetry, (Santa Barbara, California, USA), (1999).

Hinze, J. O., Turbulence, (1975), 39-58, McGraw-Hill.

Kähler, C. J., Adrian, R. J. and, Willert, C. E., Turbulent Boundary Layer Investigations with Conventional- and Stereoscopic Particle Image Velocimetry, 9th International Symposium on Applications of Laser Techniques to Fluid Mechanics (Portugal), (1998).

Marple, Jr., S. L., Digital Spectral Analysis, (1987), 149-152, Prentice-Hall Inc.

Meinhart, C.D. and Adrian, R.J., On the Existence of Uniform Momentum Zones in a Turbulent Boundary Layer, Phys. Fluids, 7 (1995), 694-696.

Piirto, M. and Saarenrinne, P., Interaction between Flocculation and Turbulence - A Method Using the Combination of Image Processing and PIV, Symposium on Optical Methods and Image Processing in Fluid Flow Measurements, ASME/JSME Fluids Engineering Conference, (San Francisco, California, USA), (1999a).

Piirto, M. and Saarenrinne, P., Turbulence Length Scale Estimation with PIV, 8th International Conference on Laser Anemometry Advances and Applications, (Rome, Italy), (1999b)

Piirto, M., Eloranta, H. and Saarenrinne, P., Interactive Software for Turbulence Analysis from PIV Vector Fields, 10th International Symposium on Applications of Laser Techniques to Fluid Mechanics, (Portugal), (2000).

Saarenrinne, P. and Piirto, M., Turbulent Kinetic Energy Dissipation rate Estimation from PIV Velocity Vector Fields, Experiments in Fluids, 29 (2000), 300-307.

Stanislas, M., Carlier, J., Foucaut, J. M. and Dupont, P., Experimental Study of a High Reynolds Number Turbulent Boundary Layer Using DPIV, 9th International Symposium on Applications of Laser Techniques to Fluid Mechanics, (Portugal), (1998).

Tomkins, C.D. and Adrian, R. J., Comparison of Energetic Spanwise Modes in a Boundary Layer and Channel, 10th International Symposium on Applications of Laser Techniques to Fluid Mechanics (Portugal), (2000).

Author Profile

Mika Piirto: He received his M.Sc. (Eng.) degree in Electrical Engineering in 1988 and his Licentiate of Technology degree 1991 (Digital Control) from Tampere University of Technology. Currently he is working as a research engineer in Energy and Process Engineering Laboratory. In the last few years his research interest has been in turbulence characterization with particle image velocimetry.

Heimo Ihalainen: He received his M.Sc. (Eng.) degree in Electrical Engineering in 1980 from Tampere University of Technology. Currently he is working as the laboratory manager of the Laboratory of Measurement and Information Technology in the same university. His research projects are in process signal analysis, multivariate analysis and measurement based on images.

Hannu Eloranta: He received his M.Sc. (Eng.) degree in Energy and Environmental Engineering in 2000 from Tampere University of Technology. Currently he is working as a Ph.D. student in the field of experimental fluid dynamics at the same university. His research work is focused on the structure of turbulence in plane and convergent channel flows.

Pentti Olavi Saarenrinne: He received his M.Sc. (Eng.) degree in Mechanical Engineering in 1976 and his Licentiate of Technology degree 1986 from Tampere University of Technology. He is working as Laboratory Manager in Energy and Process Engineering Laboratory. His research interest covers experimental fluid mechanics in internal flows (in industrial applications). He is acquainted in hot wire, laser Doppler and particle image velocimetry techniques.